ORIGINAL ARTICLE

月旦知識庫

Evaluating the potential of *Cajanus cajan* (L.) Millsp. Root to improve atopic dermatitis with different anti-inflammatory models and active compounds

Shu-Er Yang [a], Xiang-Ming Cai [b], Yu-Wen Chu [c], Jen-Chieh Tsai [d], Mey-Fann Lee [e], Tuzz-Ying Song [b,*]

[a] Department of Beauty Science and Master Program of Beauty Science and Technology, Chienkuo Technology University, Changhua, Taiwan
[b] Department of Medicinal Botanicals and Foods on Health Applications, Da-Yeh University, Taiwan, ROC
[c] Department of Pharmacy, Taichung Veterans General Hospital, Taichung, Taiwan, ROC
[d] School of Pharmacy, China Medical University, Taichung, Taiwan No. 100, Section 1, Jingmao Road, Beitun District, Taichung City 406040, Taiwan, ROC
[e] Department of Medical Research, Taichung Veterans General Hospital, Taichung, Taiwan, ROC

Abstract

Atopic dermatitis (AD) is a chronic inflammatory disease characterized by recurrent bacterial infections that cause pruritus, erythema, xerosis and thickening. *Cajanus cajan* root extract prepared with 95% ethanol (EECR95) has been shown to possess antioxidant, anti-inflammatory, and antibacterial properties in previous studies. This study aimed to evaluate EECR95's ability to improve AD by inhibiting methicillin-resistant *Staphylococcus aureus* (MRSA) growth and reducing inflammation. This study found EECR95 effectively inhibits MRSA growth (IC_{50} = 103.74 μg/mL) and reduces pro-inflammatory cytokine production in an MRSA-keratinocyte-macrophage model. LC/MS/MS analysis revealed the presence of active compounds-flavonoids, isoflavones, and flavonoid glycosides, highlighting EECR95's potential in improving atopic dermatitis *in vitro*.

Keywords: Anti-inflammatory, Atopic dermatitis, *Cajanus cajan* (L.) Millsp., Methicillin-resistant *staphylococcus aureus* (MRSA)

1. Introduction

Atopic dermatitis (AD) is a common chronic inflammatory skin disease characterized by recurrent bacterial infections, particularly *Staphylococcus aureus* (SA) [1]. AD involves skin barrier dysfunction with heterogeneous etiology and prognosis; some cases resolve spontaneously with age [2]. The severity of AD is influenced by exposure to inhalant and food allergens, air pollution, meteorological conditions, and other environmental factors, including alterations in the skin microbiota. Approximately 60%−100% of patients with AD have SA colonization on their skin, compared with 5%−30% of healthy subjects [3,4], and about 10%−30% of SA isolates from AD patients are methicillin-resistant *S. aureus* (MRSA) [5]. The incidence and prevalence of MRSA infections continue to rise worldwide [6].

Multiple factors contribute to SA colonization in AD skin, including enhanced SA adhesion to keratinocytes, reduced levels of antimicrobial peptides (AMPs), decreased filaggrin and filaggrin degradation products (FDPs), overexpression of Th2 cytokines, dysbiosis of the cutaneous microflora, and altered lipid profiles [7]. Normal skin harbors commensal bacteria such as *S. epidermidis* and *S. hominis*, which regulate skin T-cell development,

Received 7 October 2025; accepted 23 February 2026.
Available online 11 August 2026

* Corresponding author at: Department of Medicinal Botanicals and Foods on Health Applications, Da-Yeh University, Changhua 515006, Taiwan, ROC. E-mail addresses: jessica@ctu.edu.tw (S.-E. Yang), yuwenchu@vghtc.gov.tw (Y.-W. Chu), jenchieh@mail.cmu.edu.tw (J.-C. Tsai), mflee@vghtc.gov.tw (M.-F. Lee), song77@mail.dyu.edu.tw (T.-Y. Song).

https://doi.org/10.38212/2224-6614.3591
2224-6614/© 2026 Taiwan Food and Drug Administration. This is an open access article under the CC-BY-NC-ND license (http://creativecommons.org/licenses/by-nc-nd/4.0/).

月日知識庫

dampen inflammation, and prevent infection through the production of AMPs [8]. Therefore, when the microbiota becomes imbalanced, it may facilitate the development of pathogenic bacterial infections, including those caused by *S. aureus*. Patients colonized with SA also exhibit higher skin pH than non-colonized individuals, suggesting a link between skin pH and microbiota imbalance [9].

Reduced commensal bacterial diversity in AD further promotes SA colonization [10]. In addition, SA preferentially adheres to AD skin, although the mechanisms underlying this tropism are not fully understood [10]. A decrease in FDPs in the stratum corneum is associated with the formation of deformed keratinocytes, to which SA from AD skin binds with increased affinity [10,11]. Stratum corneum lipids, including free fatty acids, ceramides, and sphingosine, are also critical for maintaining the skin barrier and preventing infections such as those caused by SA [12]. Th2 cytokines, which are highly expressed in AD skin, can profoundly alter lipid metabolism and lipid composition [13].

SA colonization can establish a vicious cycle in which infection exacerbates AD by inducing thymic stromal lymphopoietin (TSLP) and promoting Th2/Th17-type inflammation [10,14]. Short amphipathic phenol-soluble modulins (PSMs), including the PSMα and PSMβ families and δ-toxin, are secreted by SA via the Pmt transporter and stimulate keratinocytes to release proinflammatory cytokines such as IL-8 and IL-1β [15]. Collectively, these findings suggest that inhibiting SA proliferation and colonization on the skin, as well as suppressing SA-induced keratinocyte inflammation, may effectively alleviate AD-associated inflammation.

Cajanus cajan (L.) Millsp. (pigeon pea), a woody annual or perennial legume [16]. Among approximately 37 species in the genus *Cajanus*, *C. cajan* is the most widely used commercial species owing to its high nutritional value and functional properties [17]. It likely originated in ancient Egypt, Africa, Asia, and the Americas, and is now widely cultivated in tropical and subtropical regions, with India accounting for about 77% of the cultivated area [18]. Various parts of *C. cajan*, including roots, leaves, and seeds, exhibit diverse biological activities [19], and *C. cajan* roots (CCR) in particular show strong antioxidant, anti-inflammatory, and antibacterial effects [20]. The *C. cajan* root extract prepared with 95% ethanol (EECR95) has been reported to exert hypoglycemic and lipid-lowering effects in rats [21]. Vo et al. [22] further demonstrated the hepatorenal protective effects of EECR95 and proposed that soy isoflavones (genistein, biochanin A, daidzein, genistin, and cajanol) are its major active constituents, estimating a safe human dose of 972 mg per 60-kg person per day.

Abbreviations

AD	atopic dermatitis
CCR	*Cajanus cajan* (L.) Millsp. Root
EECR95	95% ethanol extract of *C. cajan* root
MRSA	multi-resistant *Staphylococcus aureus*
SA	*Staphylococcus aureus*
LPS	lipopolysaccharide
AMPs	antimicrobial peptides (AMPs)
FDPs	filaggrin degradation products
TSLP	thymic stromal lymphopoietin
PSMs	phenol-soluble modules
Pmt	PSM transporter
IL	interleukin
NF-κB	nuclear factor kappa B
MIC	minimum inhibitory concentration
MBC	minimum bactericidal concentration
PMA	12-O-Tetradecanoylphorbol-13-acetate
CFU	colony forming unit
mTHP-1 cells	THP-1 cells were differentiated to macrophage-like cells induced by PMA
VFs	virulence factors
TNFAIP3	tumor necrosis factor alpha-induced protein 3
GPER	protein-coupled estrogen receptor
TEWL	trans-epidermal water loss

Our previous work showed that the anti-inflammatory activity of EECR95 is mainly mediated through activation of the nuclear factor (NF)-erythroid 2-related factor 2/heme oxygenase-1 (Nrf2/HO-1) pathway and inhibition of the nuclear factor kappa B (NF-κB) signaling pathway, thereby conferring antioxidant and anti-inflammatory effects [23]. The main aim of the present study was to evaluate whether EECR95 has the potential to ameliorate AD. To this end, we employed three inflammatory models [lipopolysaccharide (LPS)-induced and MRSA-induced macrophage inflammation, both directly and indirectly] to identify the most suitable *in vitro* system for assessing AD-related effects of EECR95. In addition, LC-MS/MS-Q-TOF analysis was used to refine the phytochemical profiling of EECR95 and identify further potential bioactive compounds. Therefore, we hypothesized that EECR95 can inhibit SA/MRSA growth and attenuate LPS- and MRSA-induced inflammatory responses relevant to AD pathogenesis. To this end, we employed three inflammatory models to identify a suitable *in vitro* system for evaluating AD-related effects of EECR95.

月日知識庫

2. Materials and methods

2.1. Chemicals

The roots of *C. cajan* (Taitung No. 3) were dug out after harvest, washed, and sun-dried for about 5 days. They were then cut into 5-cm segments to obtain the CCR sample, which was kindly provided by Dr. Chen-Yi Chen (Taitung District Agricultural Research and Extension Station, Council of Agriculture, Executive Yuan, ROC). 12-O-Tetradecanoylphorbol-13-acetate (PMA, P8139) was purchased from the Sigma Chemical Co. (St. Louis, MO, USA). The ethanol and acetone solvents were HPLC grade (Fisher Scientific Co.). Lipopolysaccharide (LPS; *Escherichia coli* O26:B6) and bovine serum albumin were bought from Sigma–Aldrich Co. (St Louis, MO, USA). Dulbecco's modified Eagle's medium (DMEM), fetal bovine serum (FBS) from Gibco by Life Technologies (Frederick, MD, USA). Chemicals and reagents are of high quality. Tips, dishes, test tubes, etc., for cell culture were bought from Thermo Fisher Scientific (Waltham, MA, USA).

2.2. Preparation of hot water and ethanol extracts of C. cajan roots (CCR)

CCR was rinsed with running water to remove the soil. The surface of the CCR was sterilized in 95% ethanol for 3 min and then rinsed thrice in sterile distilled water. The surface-sterilized CCR was milled into powder. A portion of the CCR powder was extracted with a 1:20 ratio (w/v) of 97 °C ± 2 °C hot water for 3 h, or extracted with 1:20 50%, 75%, and 95% ethanol by soaking at room temperature for 72 h. After filtering through Whatman No. 2 filter paper, the filtrates were concentrated (10-fold) under reduced pressure and lyophilized to obtain the hot water (HWCR) and 50%, 75%, and 95% ethanol extract of CCR (EECR50, EECR75 EECR95). The extraction yields of HWCR, EECR50, EECR75, and EECR95 were 8.7, 7.5, 4.3 and 3.1%, respectively.

2.3. Cell culture and cell anti-proliferative assay

THP-1 cell line (Human leukemia monocytic cell line; BCRC60430) was purchased from the Bioresource Collection and Research Center at the Food Industry Research and Development Institute (Hsinchu, Taiwan). THP-1 cells were cultured in RPMI 1640, supplemented with 10% FBS, 2 g/L sodium bicarbonate, 1% penicillin/streptomycin (Life Technologies, USA) at 37 °C in a 5% CO_2 incubator. HGF-1 cell line (Human Gingival fibroblasts cells; ATCC®CRL-2014 Manassas, VA, United States) was cultured in the low glucose Dulbecco's Modified Eagle Medium (DMEM; glucose 1 g/L) (Gibco, Thermo Fisher Scientific, MA, United States) supplemented with 10% (v/v) FBS and 1% (v/v) 200 mM L-glutamine (Gibco, Thermo Fisher Scientific, MA, United States) at 37 °C in a 5% CO_2 incubator.

The medium was changed every two days. Cells were seeded at a density of 1×10^5 cells/well into a 12-well plate 24 h before treatment. After incubation, cells were washed twice with PBS × 1 and lysed with trypsin EDTA 0.25% (Gibco, CAD). The morphological changes were observed with an inverted microscope (AE3145, Beijing, China). The trypan blue exclusion method was used to determine the number of viable cells at 24, 48, and 72 h incubation using a hemocytometer.

The cytotoxicity of HWCR, EECR50, 70 and 95 on THP-1 cells was determined by the MTT assay described in Vo et al. [23]. Cells were treated with various sample concentrations (0–500 μg/mL), and cell viability was detected at 570 nm using an ELISA reader (Synergy HTX, BioTek, Winooski, VT, USA).

2.4. Microorganisms and culture medium

MRSA was generously provided by Dr. Mey-Fann Lee (Taichung Veterans General Hospital, Taiwan). The bacteria were stored on agar slants at 4 °C and subcultured overnight at 35 °C on Mueller-Hinton agar slants. The bacterial growth was harvested using 5 mL of sterile Nutrient broth, and its absorbance was measured at 550 nm. The suspension was then diluted to achieve a viable cell count of 10^7 CFU/mL using a spectrophotometer.

2.5. Antibacterial activity of ethanol extract of C. cajan

2.5.1. Preparation of bacterial culture

Bacteria were cultured in 5 mL tubes at 37 °C. After overnight incubation, the bacterial cultures were diluted in broth to a final concentration of 5×10^5 CFU/mL. A two-fold dilution series of test samples and fractions in 0.1 mL of PBS was placed into wells of flat-bottomed microtiter plates (Nunc 96-well flat-bottomed microtiter plates). A 10 μL volume of bacterial culture was then added. After incubating the plates at 37 °C for 24 h, the minimum inhibitory concentration (MIC) and minimum bactericidal concentration (MBC) were determined as described previously [24].

日日知識庫

2.5.2. MIC determination [24]

All the extracts were assayed for their antibacterial activities in a standard MIC assay. The MICs were recorded as the lowest concentration or dilution of the test sample or fraction that completely inhibited visible growth of the bacteria.

2.5.3. MBC determination [24]

From tubes showing no visible growth (those at or above the MIC concentration), small aliquots are aseptically taken and plated onto Nutrient agar medium without the antimicrobial agent. Then, the plates are incubated at 37 °C for 24 h. After incubation, the plates are examined for bacterial growth. The MBC is defined as the lowest concentration of the antimicrobial agent that results in no bacterial growth on the agar plates (kills ≥99.9% of the bacterial population). The MBC test distinguishes between bacteriostatic (growth-inhibiting) and bactericidal (killing) activity. A smaller difference between the MIC and MBC values indicates a stronger bactericidal effect. Conversely, the greater the difference between the MIC and MBC values, the more it indicates a tendency to inhibit bacterial growth.

2.5.4. Disk-diffusion method [25]

Paper disks (0.6 cm diameter) impregnated with samples of different concentrations were placed on MRSA-seeded agar plates. After standing for 3–5 min, the plates were incubated at 37 °C for 24 h, and the diameters of the inhibition zones were measured to evaluate antibacterial activity. HWCR extracts were tested at 0.25–1.0 mg/disc, whereas EECR50, EECR70, and EECR95 were tested at 0.01–0.5 mg/disc.

2.6. PMA induction of THP-1 cell assay

This method was based on the method of Koganti et al. [26] with some modifications. THP-1 monocytes are differentiated into macrophages by 24 h incubation with 100 nM PMA followed by 24 h incubation in RPMI medium. PMA-induced differentiation of macrophage-like THP-1 cells, abbreviated as mTHP-1 cells.

2.7. Anti-inflammation model establishment

2.7.1. LPS-direct induce mTHP-1 inflammation

mTHP-1 cells (2×10^5 cells/well) were seeded into 24-well plates and incubated for 24 h. Subsequently, varying concentrations of EECR95 (10–40 μg/mL) were added to the wells before stimulation with LPS (1 μg/mL) for 2 h, followed by an additional 24 h incubation. After the treatment, the culture medium was collected, and the supernatant was analyzed for cytokine levels, including IL-1β, IL-6, and TNF-α, using ELISA kits according to the manufacturer's instructions (Invitrogen Co., Camarillo, CA, USA).

2.7.2. MRSA-direct induce mTHP-1 inflammation

10 μL of MRSA with an absorbance value of 0.1 (bacterial count of 1.69×10^4) and EECR95 (10–40 μg/mL) were co-incubated with mTHP-1 for 1 h of incubation. Then, the supernatant was filtered through a 0.22 μm filter and measured for cytokines (including IL-1β, IL-6, and TNF-α) using ELISA kits.

2.7.3. MRSA-indirect induce mTHP-1 inflammation

A 10 μL suspension of MRSA, with an absorbance value of 0.1 (corresponding to a bacterial count of 1.69×10^4), was co-incubated with HaCaT cells (human keratinocytes) for 12 h. Following incubation, 50 μL of the supernatant was collected after filtration (0.22 μm), and EECR95 (at concentrations ranging from 10 to 40 μg/mL) was added to mTHP-1 cells for a subsequent 24-h incubation. Then, the supernatant was filtered through a 0.22 μm filter and measured for cytokines (including IL-1β, IL-6, and TNF-α) using ELISA kits.

2.8. Quantitative real-time PCR

This method was adapted from Lee et al. [27] with minor modifications. HaCaT cells (2.5×10^5 cells/mL) were seeded in 6-well plates for 24 h, serum-starved for 16 h, and pretreated with EECR95 (1.25–10 μg/mL) for 2 h. MRSA (10 μL, OD = 0.1) was then added and incubated for 1 h. Supernatants were passed through a 0.22 μm filter, and total RNA from filtrates and cells was extracted using TRIzol (Invitrogen). cDNA was synthesized using the SuperScript III kit (Invitrogen), and quantitative real-time PCR was performed on a StepOnePlus™ system (Applied Biosystems) using primers listed in Table 1. Gene expression was normalized to GAPDH and expressed as fold change relative to medium-only controls.

2.9. Untargeted analysis of phytochemicals by LC-MS/MS Q-TOF

Samples were separated on an ultraperformance liquid chromatography system (1260 Infinity II, Agilent) with an Atlantic T3 column (3 μm, 2.1 mm × 10 cm). The mobile phase consisted of 0.1% formic acid (FA) in water (A) and 0.1% FA in

月日知識庫

Table 1. Oligonucleotide primers used for real-time PCR.

PCR product (Size)	Forward (5′ to 3′)	Reverse (5′ to 3′)
IL-1α (248 bp)	AAGACAAGCCTGTGTTGCTGAAGG	TCCCAGAAGAAAATGAGGTCGGTC
IL-17 (204 bp)	TGAATTTCTGCCCTTCCCATT	GGTTCAGGGGTGACACCATTT
GM-CSF (265 bp)	GCTGCTGAGATGAATGAAAC	AGTCAAAGGGGATGACAAG
GAPDH (201 bp)	GAGTCAACGGATTTGGTCGT	TGGGATTTCCATTGATGACA

acetonitrile (B). The gradient was adapted from López-Fernández et al. [28], and the detailed conditions are shown in [Supplementary Fig. 1] (https://doi.org/10.38212/2224-6614.3591). Samples were analyzed in both positive and negative ion modes on a Q-TOF mass spectrometer (TripleTOF 6600, Sciex) using data-dependent acquisition. TOF-MS and MS/MS scan ranges were m/z 100–1000 and 50–1000, respectively. Compounds were identified with PeakView 2.2, using a similarity score >70% between predicted and experimental fragment spectra as the identification criterion.

2.10. Statistical analyses

Data are presented as mean ± SD from three independent experiments (n = 3). Statistical analyses were performed using SPSS software (version 22). Differences among groups were evaluated by one-way ANOVA followed by Duncan's multiple range test. A p-value <0.05 was considered statistically significant. In the figures, columns that do not share a common letter differ significantly at $p < 0.05$.

3. Results

3.1. Antiproliferative effects of CCR extracts

3.1.1. Antiproliferative effects of CCR extracts on cells

As shown in Fig. 1 (A), increasing the concentration of each extract resulted in a decrease in the cell survival rate, demonstrating a significant dose-dependent inhibition effect. At a concentration of 500 μg/mL, the survival rates of all extracts, except HWCR (>90%), were <90%. The inhibitory effects of the extracts on cell proliferation followed the order EECR95 > EECR70 > EECR50, with EECR95 exhibiting the strongest inhibitory effect (Fig. 1 (A)).

To confirm a non-toxic concentration for the antimicrobial test, EECR95 was added at concentrations ranging from 10 to 500 μg/mL and incubated for 24–72 h. The study revealed that as the concentration of EECR95 increased, the inhibition of cell proliferation became progressively more pronounced. At a concentration of 500 μg/mL, cell proliferation was almost completely inhibited; however, no cytotoxicity was observed, as the cell count did not fall below the original number (7.8×10^4) (Fig. 1 (B)).

3.1.2. Anti-bacterial effects of C. cajan root extracts on MRSA

Fig. 2 illustrates the antibacterial effects of different concentrations of ethanol extracts from *CCR* (Fig. 2(A)). By calculating the diameter of the inhibition zones, it was observed that EECR95 exhibited a dose-dependent inhibition of SA growth at doses below 0.5 mg, with an inhibition zone diameter of 1.8 cm/disc. EECR70 and EECR50 followed, with inhibition zones of 1.2 cm/disc and 1.0 cm/disc, respectively (Fig. 2(B)). Consequently, further analysis of the MIC and MBC values of EECR50, EECR70, and EECR95 was conducted.

From the results in Table 2, it was found that EECR95 had lower MIC and MBC values compared to EECR50 (450 and 650 μg/mL) and EECR70 (250 and 450 μg/mL), with values of 120 and 225 μg/mL, respectively. This indicates that the antibacterial efficacy follows the order of EECR95 > EECR70 > EECR50 against SA. However, the antibacterial activity of EECR95 was far inferior to that of the genistein standard (120 and 225 μg/mL) and the antibiotic ampicillin (120 and 225 μg/mL).

3.1.3. Anti-bacterial effects of EECR95 and ampicillin on SA and MRSA

The results of Fig. 3(A) showed that EECR95 showed a tendency to significantly inhibit the growth of SA after co-incubation with MRSA at concentrations of 12.5–200 μg/mL for 24 h. It also had a concentration effect, with an IC_{50} of about 93.25 μg/mL. However, its inhibitory effect was not as strong as that of Ampicillin (IC_{50} = 30.15 μg/mL). In contrast, Ampicillin had no inhibitory effect on MRSA at all, while EECR95 still had a significant inhibitory effect (IC_{50} = 103.74 μg/mL) (Fig. 3(B)).

月旦知識庫

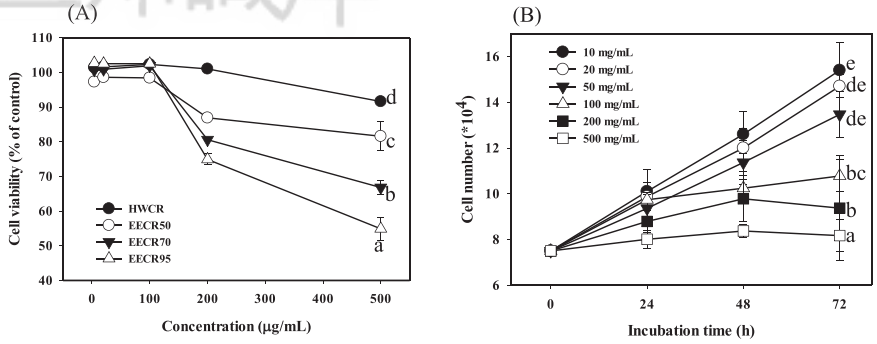

(a) **Cell viability (24 h incubation)** (b) **Cell proliferation (24 -72h incubation)**

Fig. 1. Effects of C. cajan root extracts on THP-1 cell viability and proliferation. The cell viability of THP-1 cells cultured for 24 h with different concentrations of C. cajan root extract prepared with hot water (HWCR) and 50%, 70%, or 95% ethanol (EECR50, 70 and 95) at 10–500 μg/mL (A), and the inhibition of THP-1 cell proliferation with different concentrations of EECR95 (10–500 μg/mL) at 24–72 h incubation time (B). Cell viability was assessed using the MTT assay. Cell proliferation was measured using the Trypan blue exclusion assay. Data are presented as mean ± SD (n = 3). Groups that do not share the same superscript letter are significantly different (p < 0.05, one-way ANOVA followed by Duncan's multiple range test).

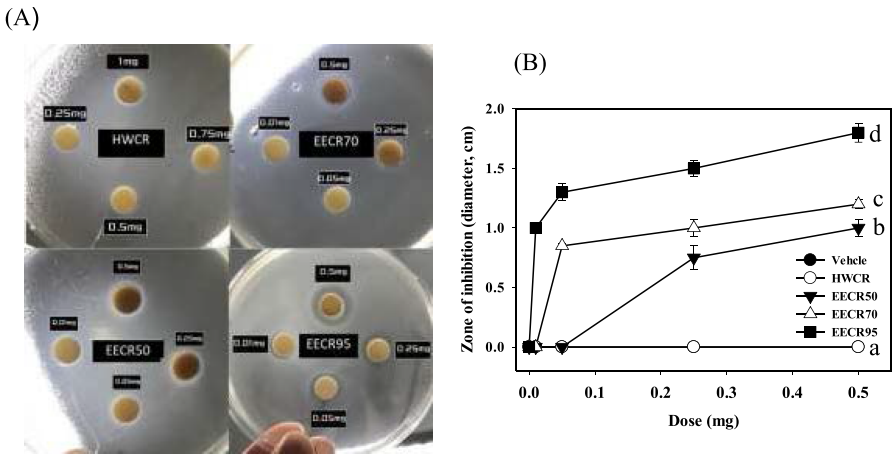

Fig. 2. Antibacterial activity of Cajanus cajan root ethanol extracts against Staphylococcus aureus (SA). (A) Agar diffusion assay: paper disks containing C. cajan root extract prepared with hot water (HWCR) and 50%, 70%, or 95% ethanol (EECR50, EECR70 and EECR95) were placed on agar plates inoculated with SA, and inhibition zones were observed after incubation. (B) Inhibition zones: diameters of the inhibition zones were measured to quantify antibacterial activity. Data are presented as mean ± SD (n = 3). Groups that do not share the same superscript letter are significantly different (p < 0.05, one-way ANOVA followed by Duncan's multiple range test).

Table 2. Minimum inhibitory concentration (MIC) and minimum bactericidal concentration (MBC) of ethanol extracts of C. cajan root (EECR-50, EECR-70, and EECR-95) against Staphylococcus aureus (SA) after 24 h of incubation.

Samples	*Staphylococcus aureus (SA)* (μg/mL)	
	MIC[b]	MBC
Ampicillin	0.5	1.0
Genistein	10	25
EECR-50[a]	450	650
EECR-70	250	450
EECR-95	120	225

[a] EECR50, 70 and 95: EECR-50, 70 and 95% ethanol of *C. cajan* roots.
[b] MIC and MBC values are representative of three independent experiments.

3.2. Cell viability of EECR-95 and genistein in mTHP-1

To ensure that the subsequent anti-inflammatory test will not result in incorrect anti-inflammatory interpretation due to the decrease in cell number caused by cytotoxicity, it is necessary to select a concentration that does not have cytotoxicity (Cell viability>90%) for the test. Based on the results shown in Fig. 4, the working concentration of genistein should be kept below 20 μg/mL, whereas that of EECR95 should be kept below 40 μg/mL in mTHP-1 cells, so as to avoid apparent cytotoxicity while still eliciting clear biological effects for the subsequent anti-inflammatory experiments.

月旦知識庫

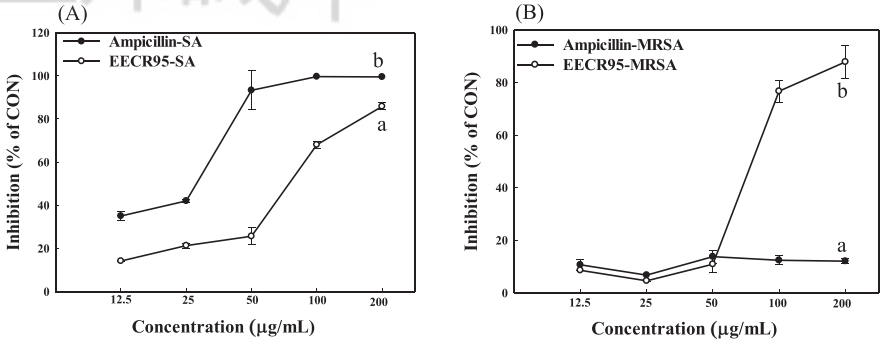

(**a**) *Staphylococcus aureus* (SA)

(**b**) Multiple-resistant *Staphylococcus aureus* (MRSA)

Fig. 3. Inhibitory effects of C. cajan root extract prepared with 95% ethanol (EECR95) and ampicillin on the growth of Staphylococcus aureus (SA) (A) and methicillin-resistant S. aureus (MRSA) (B) after 24 h incubation at different concentrations (12.5–200 μg/mL). Data are presented as mean ± SD (n = 3). Within each treatment, values not sharing the same lowercase letter are significantly different (p < 0.05, one-way ANOVA followed by Duncan's multiple range test).

3.3. Evaluation of anti-AD effects of EECR95

3.3.1. Model 1: LPS-induced inflammation in mTHP-1

In the LPS-induced mTHP-1 cell model (Table 3), LPS (CON) markedly increased IL-1β, IL-6, and TNF-α compared with the blank group (IL-1β: 318.85–643.46 pg/mL; IL-6: 1.69–9.13 ng/mL; TNF-α: 5.10–19.32 ng/mL). Genistein (10 μg/mL) significantly reduced these cytokines, with inhibition rates of 66.04% (IL-1β), 120.70% (IL-6), and 89.73% (TNF-α). EECR95 (10–40 μg/mL) dose-dependently suppressed IL-1β, lowering it to 380.22–290.92 pg/mL (0.5909–0.4521-fold vs. LPS control;

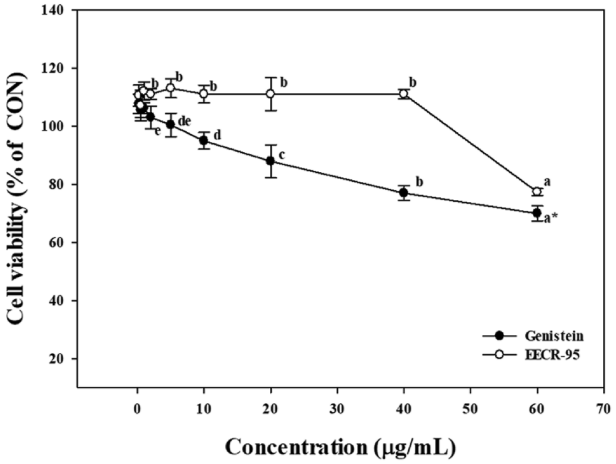

Fig. 4. Effects of C. cajan root extract prepared with 95% ethanol (EECR95) and genistein on the viability of mTHP-1 cells after 24 h incubation. Cell viability is expressed as a percentage of the untreated control (CON). Data are presented as mean ± SD (n = 3). Within each treatment (EECR-95 or genistein), values not sharing the same lowercase letter are significantly different (p < 0.05, one-way ANOVA followed by Duncan's multiple range test).

Table 3. Effects of different concentrations of C. cajan root extract prepared with 95% ethanol (EECR95) on cytokine production in mTHP-1 cells induced by LPS.

Treatment	Cytokine levels	Fold vs CON[3]	Inhibition (%)[4]
IL-1β (pg/mL)[2]			
Blank	318.85 ± 4.67[b,5]	0.6668	
CON (LPS, 1 μg/mL)[1]	643.46 ± 1.42[f]	1	
+ Gen (10 μg/mL)	429.09 ± 4.05[e]	0.6668	66.04
+ EECR95 (10 μg/mL)	380.22 ± 2.50[d]	0.5909	81.09
+ EECR95 (20 μg/mL)	350.84 ± 3.21[c]	0.5452	90.15
+ EECR95 (40 μg/mL)	290.92 ± 1.89[a]	0.4521	108.60
IL-6 (ng/mL)			
Blank	1.69 ± 0.11[b,4]	0.1851	
CON (LPS, 1 μg/mL)	9.13 ± 0.15[f]	1	
+ Gen (10 μg/mL)	0.15 ± 0.04[a]	0.0165	120.70
+ EECR95 (10 μg/mL)	8.77 ± 0.09[e]	0.9606	4.84
+ EECR95 (20 μg/mL)	7.70 ± 0.17[d]	0.8434	19.22
+ EECR95 (40 μg/mL)	6.17 ± 0.19[c]	0.6758	39.78
TNF-α (ng/mL)			
Blank	5.10 ± 0.14[a]	0.2640	
CON (LPS, 1 μg/mL)	19.32 ± 0.14[e]	1	
+ Gen (10 μg/mL)	6.56 ± 0.16[b]	0.3396	89.73
+ EECR95 (10 μg/mL)	13.14 ± 0.18[d]	0.6801	43.46
+ EECR95 (20 μg/mL)	10.84 ± 0.21[c]	0.5611	59.63
+ EECR95 (40 μg/mL)	4.84 ± 0.16[a]	0.2505	101.83

[1] mTHP-1 cells were pretreated with EECR95 (1–40 μg/mL), Gen (genistein; 10 μg/mL) for 2 h and then incubated with lipopolysaccharide (1 μg/mL) for 24 h.

[2] Interleukin-1 (IL-1α), interleukin-6 (IL-6), and tumor necrosis factor-α (TNF-α) levels were determined by ELISA kits.

[3] Fold vs CON = cytokine level of each treatment/LPS-induced control (CON).

[4] Inhibition (I)% = [(LPS induction group −Sample group)/(LPS induction group −Blank group)] × 100%. Values exceeding 100% indicate that the cytokine level in the treated group is lower than that of the blank group.

[5] Data are presented as mean ± SD (n = 3). Values that do not share the same lowercase letter are significantly different (p < 0.05, one-way ANOVA followed by Duncan's multiple range test). One-way ANOVA revealed significant treatment effects for IL-1β ($F_{5,12}$ = 56.3, $p < 0.001$), IL-6 ($F_{5,12}$ = 41.7, $p < 0.001$), and TNF-α ($F_{5,12}$ = 89.2, $p < 0.001$).

日日知識庫

81.09–108.60% inhibition). For IL-6, EECR95 produced weaker but concentration-dependent inhibition, reducing levels to 8.77–6.17 ng/mL (0.9606–0.6758-fold; 4.84–39.78% inhibition). TNF-α was decreased to 13.14, 10.84, and 4.84 ng/mL at 10, 20, and 40 μg/mL EECR95 (0.6801–0.2505-fold), with inhibition rates of 43.46%, 59.63%, and 101.83%, indicating that high-dose EECR95 (40 μg/mL) suppressed TNF-α more effectively than genistein.

3.3.2. Model 2: MRSA coculture with mTHP-1-induced inflammation

To confirm the ability of EECR95 to inhibit the inflammation in MRSA-induced macrophages directly, MRSA was used to induce the inflammatory response in differentiated mTHP-1 cells. The relationship between turbidity ($OD_{550\ nm}$) and bacterial cell number was first established, enabling the conversion of turbidity measurements into actual bacterial counts. The results in [Supplementary Fig. 2] (https://doi.org/10.38212/2224-6614.3591) show a strong linear correlation ($R^2 = 0.99$) between MRSA counts (0–1.5 × 10^7 CFU/mL) and turbidity (0–0.8).

Fig. 5 shows that the viability of mTHP-1 cells significantly decreased with increasing co-culture time with MRSA, dropping to about 40% of the initial level after 6 h. To maintain mTHP-1 cell viability above 90%, a 1-h co-culture period with MRSA was selected to induce cellular inflammation.

In the MRSA co-culture mTHP-1 cell model (Table 4), MRSA-induced mTHP-1 (CON) markedly increased IL-1β and TNF-α compared with the blank group (IL-1β: 0.65–8.56 pg/mL; TNF-α: 64.19–125.67 ng/mL). Genistein (10 μg/mL) significantly reduced IL-1β and TNF-α to 1.56 and 66.67 pg/mL ($P < 0.05$), corresponding to 0.1822- and 0.5305-fold of the MRSA control, with inhibition rates of 88.50% and 95.97%. In contrast, EECR95 (10–40 μg/mL) showed no inhibition of IL-1β (8.59–8.58 pg/mL; 1.0035–1.0023-fold; −0.38% to −0.25% inhibition) and only weakly reduced TNF-α (120.11–111.96 pg/mL; 0.9558–0.8909-fold; 9.04–22.30% inhibition), much less effectively than genistein. IL-6 was not detected in any group.

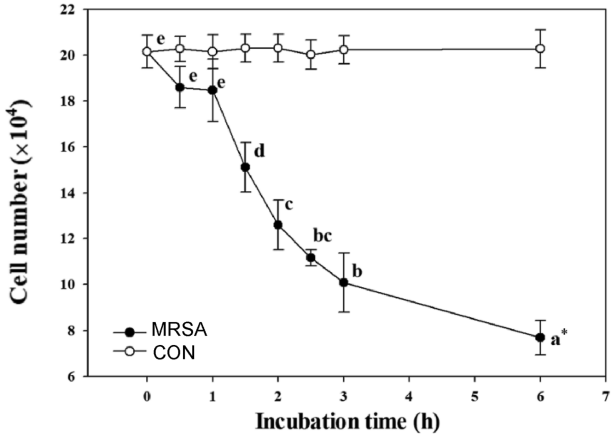

Fig. 5. Changes in the cell number of methicillin-resistant Staphylococcus aureus (MRSA) co-cultured with PMA-stimulated mTHP-1 cells (100 nM) for 6 h. Data are presented as mean ± SD (n = 3). Values that do not share the same lowercase letter are significantly different (p < 0.05, one-way ANOVA followed by Duncan's multiple range test).

3.3.3. Model 3: MRSA coculture with HaCaT-induced inflammation indirectly (MRSA-induced inflammation by mimicking infection of skin cells)

We first infected human keratinocytes (HaCaT) with MRSA to mimic MRSA-induced AD. The pro-inflammatory factors (culture supernatant) released from MRSA-infected HaCaT cells were then used to elicit a marked inflammatory response in mTHP-1 cells (Table 5).

In the MRSA-indirectly induced mTHP-1 cell model, MRSA (CON) increased IL-1β from 255 to 3192 pg/mL, IL-6 from 1.32 to 20.00 ng/mL, and TNF-α from 8.53 to 71.71 ng/mL. Genistein (10 μg/mL) reduced IL-1β, IL-6, and TNF-α to 1116, 4.25, and 28.10, corresponding to 0.3496-, 0.2125-, and 0.3919-fold of the MRSA control, with inhibition rates of 70.68%, 84.31%, and 69.03%, respectively. EECR95 showed a dose-dependent effect: at 40 μg/mL, IL-1β decreased to 1765 pg/mL (0.5529-fold; 48.59% inhibition), IL-6 to 3.50 ng/mL (0.1750-fold; 88.33% inhibition), and TNF-α to 16.76 ng/mL (0.2337-fold; 86.97% inhibition). Notably, EECR95 at 20–40 μg/mL inhibited TNF-α to 0.3164–0.2337-fold of the MRSA control (77.59–86.97% inhibition), exceeding the effect of genistein (Table 5).

3.3.4. Comparison of inflammatory responses produced by three different induction models

Fig. 6 results show that in Model 2, the production levels of IL-1β, IL-6, and TNF-α in both the blank group and the control group are the lowest among the three models. This indicates that directly co-culturing MRSA with mTHP-1 is not an appropriate model for evaluating AD. In contrast, the control group in Model 3 exhibits the highest production levels of IL-1β, IL-6, and TNF-α, with a more significant difference compared to the blank group ($P < 0.05$).

3.4. Effects of EECR95 on mRNA expression of IL-1α, IL-17, and GM-CSF in MRSA-stimulated HaCaT cells (real-time PCR)

To further understand whether MRSA could stimulate HaCaT cells to produce inflammatory

月旦知識庫

Table 4. Effects of C. cajan root extract prepared with 95% ethanol (EECR95) on cytokine production in MRAS co-cultured with mTHP-1 cells model.

Treatment	Cytokine levels	Fold vs CON[3]	Inhibition (%)[4]
IL-1β (pg/mL)[2]			
Blank	0.65 ± 0.11[a,5]	0.0759	
MRSA-induced mTHP-1 (CON)[1]	8.56 ± 0.05[c]	1	
+ Gen (10 μg/mL)	1.56 ± 0.05[b]	0.1822	88.50
+ EECR95 (10 μg/mL)	8.59 ± 0.02[c]	1.0035	−0.3793
+ EECR95 (20 μg/mL)	8.58 ± 0.01[c]	1.0023	−0.2528
+ EECR95 (40 μg/mL)	8.58 ± 0.04[c]	1.0023	−0.2528
IL-6 (ng/mL)			
Blank	ND	ND	ND
MRSA-induced mTHP-1 (CON)	ND	ND	ND
+ Gen (10 μg/mL)	ND	ND	ND
+ EECR95 (10 μg/mL)	ND	ND	ND
+ EECR95 (20 μg/mL)	ND	ND	ND
+ EECR95 (40 μg/mL)	ND	ND	ND
TNF-α (ng/mL)			
Blank	64.19 ± 1.89[a]	0.5108	
MRSA-induced mTHP-1 (CON)	125.67 ± 2.40[e]	1	
+ Gen (10 μg/mL)	66.67 ± 0.05[b]	0.5305	95.97
+ EECR95 (10 μg/mL)	120.11 ± 0.91[d]	0.9558	9.04
+ EECR95 (20 μg/mL)	117.89 ± 1.81[d]	0.9381	12.65
+ EECR95 (40 μg/mL)	111.96 ± 1.89[c]	0.8909	22.30

[1] mTHP-1 cells (macrophage-like cells) were differentiated from THP-1 human monocytes by stimulation with 100 nM PMA for 24 h. Differentiated mTHP-1 cells were then treated with EECR95 (10–40 μg/mL) for 24 h, followed by exposure to MRSA (1.69×10^4 CFU) for 1 h.
[2] Interleukin-1 (IL-1α), interleukin-6 (IL-6), and tumor necrosis factor-α (TNF-α) levels were determined by ELISA kits.
[3] Fold vs CON = cytokine level of each treatment/CON.
[4] Inhibition (I) % = [(CON group −Sample group)/(CON group −Blank group)] × 100%.
[5] Data are presented as mean ± SD (n = 3). Values that do not share the same lowercase letter are significantly different ($p < 0.05$, one-way ANOVA followed by Duncan's multiple range test). One-way ANOVA revealed significant treatment effects for IL-1β ($F_{5,12} = 130.4, p < 0.001$) and TNF-α ($F_{5,12} = 52.7, p < 0.001$).

Table 5. Effects of C. cajan root extract prepared with 95% ethanol (EECR95) on cytokine production in the MRSA indirectly induced mTHP-1 cells model.

Treatment	Cytokine levels	Fold vs CON[3]	Inhibition (%)[4]
IL-1β (pg/mL)[2]			
Blank	255 ± 10[a,5]	0.0799	
MRSA- indirectly induced mTHP-1 (CON)[1]	3192 ± 85[e]	1	
+ Gen (10 μg/mL)	1116 ± 122[b]	0.3496	70.68
+ EECR95 (10 μg/mL)	3183 ± 88[e]	0.997	0.30
+ EECR95 (20 μg/mL)	2776 ± 62[d]	0.8697	14.16
+ EECR95 (40 μg/mL)	1765 ± 51[c]	0.5529	48.59
IL-6 (ng/mL)			
Blank	1.32 ± 0.30[a]	0.0660	
MRSA- indirectly induced mTHP-1 (CON)	20.00 ± 0.40[a]	1	
+ Gen (10 μg/mL)	4.25 ± 0.32[b]	0.2125	84.31
+ EECR95 (10 μg/mL)	10.5 ± 0.46[c]	0.5250	50.86
+ EECR95 (20 μg/mL)	3.5 ± 0.51[b]	0.1750	88.33
+ EECR95 (40 μg/mL)	3.5 ± 0.18[b]	0.1750	88.33
TNF-α (ng/mL)			
Blank	8.53 ± 0.29[a]	0.1190	
MRSA- indirectly induced mTHP-1 (CON)	71.71 ± 7.20[d]	1	
+ Gen (10 μg/mL)	28.10 ± 0.64[c]	0.3919	69.03
+ EECR95 (10 μg/mL)	64.45 ± 3.29[d]	0.8988	11.49
+ EECR95 (20 μg/mL)	22.69 ± 2.12[bc]	0.3164	77.59
+ EECR95 (40 μg/mL)	16.76 ± 1.85[b]	0.2337	86.97

[1] mTHP-1 cells (macrophage-like cells) were differentiated from THP-1 human monocytes by stimulation with 100 nM PMA for 24 h. HaCaT cells (1×10^5) were infected with 10 μL of MRSA ($OD_{550} = 0.1$) for 24 h, and the infected culture supernatant (50 μL) was then added to mTHP-1 cells (2×10^5) that had been pretreated with EECR95 (10–40 μg/mL) for 24 h.
[2] Interleukin-1 (IL-1α), interleukin-6 (IL-6), and tumor necrosis factor-α (TNF-α) levels were determined by ELISA kits.
[3] Fold vs CON = cytokine level of each treatment/CON.
[4] Inhibition (I) % = [(CON group −Sample group)/(CON group −Blank group)] × 100%.
[5] Data are presented as mean ± SD (n = 3). Values that do not share the same lowercase letter are significantly different ($p < 0.05$, one-way ANOVA followed by Duncan's multiple range test). One-way ANOVA showed significant treatment effects for IL-1β ($F_{5,12} = 145.2, p < 0.001$), IL-6 ($F_{5,12} = 98.6, p < 0.001$), and TNF-α ($F_{5,12} = 72.3, p < 0.001$).

月旦知識庫

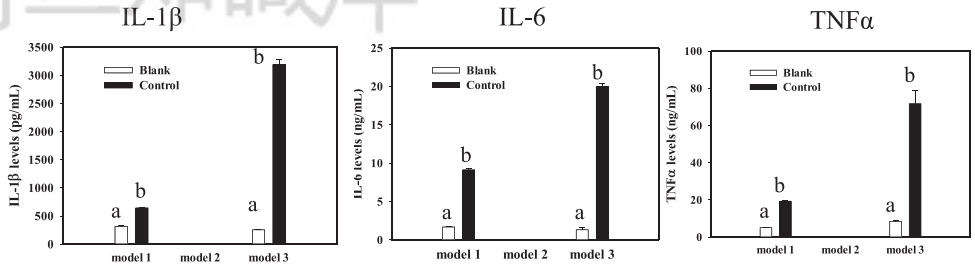

Fig. 6. Comparison of the inflammatory response in mTHP-1 cells among models 1, 2, and 3, as indicated by IL-1β, IL-6, and TNF-α production induced by methicillin-resistant Staphylococcus aureus (MRSA). Data are presented as mean ± SD (n = 3). Values that do not share the same lowercase letter are significantly different (p < 0.05, one-way ANOVA followed by Duncan's multiple range test).

responses, the mRNA expression of pro-inflammatory factors (IL-1α, IL-17, GM-CSF) was further analyzed. Fig. 7 shows that MRSA significantly induced the mRNA expression of IL-1α, IL-17, and GM-CSF (59-, 142-, and 6.6-fold increases, respectively), while EECR95 significantly inhibited the production of pro-inflammatory factors. Still, the inhibitory effects of each concentration (1.25–10 μg/mL) did not reach a significant difference ($P > 0.05$), and the inhibition rates ranged from 52% to 67%.

3.5. Untargeted analysis of phytochemicals by LC-MS/MS Q-TOF

The untargeted analysis of phytochemicals in EECR95 was conducted using LC-MS/MS Q-TOF. The total ion chromatograms (TICs) of EECR95 were obtained in both positive and negative ion modes [Supplementary Fig. 3] (https://doi.org/10.38212/2224-6614.3591). In the positive ion mode [Supplementary Fig. 3A] (https://doi.org/10.38212/2224-6614.3591), multiple peaks were observed,

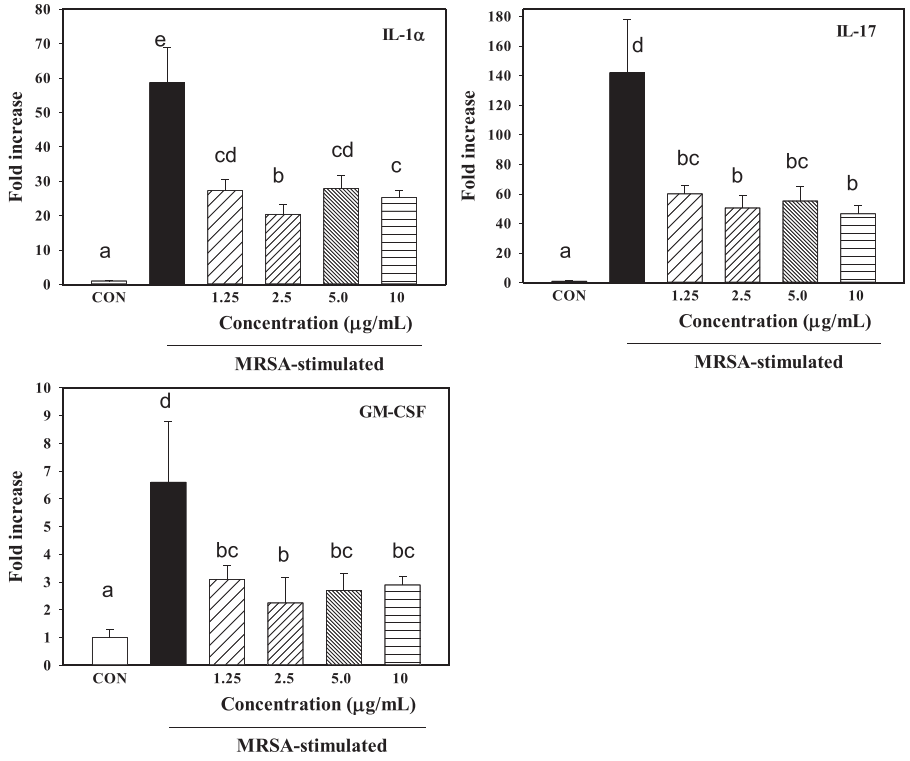

Fig. 7. Effects of different concentrations of C. cajan root extract prepared with 95% ethanol (EECR95) on the mRNA expression of IL-1α, IL-17, and GM-CSF in MRSA-stimulated HaCaT cells. Data are presented as mean ± SD (n = 3). Values that do not share the same lowercase letter are significantly different (p < 0.05). One-way ANOVA showed significant treatment effects for IL-1α ($F_{5,12} = 23.5, p < 0.0001$), IL-17 ($F_{5,12} = 17.2$, $p = 0.00003$), and GM-CSF ($F_{5,12} = 9.8, p = 0.0008$).

月日知識庫

indicating the presence of diverse phytochemical compounds. Similarly, the negative ion mode [Supplementary Fig. 3B] (https://doi.org/10.38212/2224-6614.3591) revealed distinct peaks that represent additional compounds, further confirming the complexity of the phytochemical profile of EECR95. These results suggest that EECR95 contains a wide range of bioactive compounds, which may contribute to its observed antibacterial and anti-inflammatory activity.

EECR95 was analyzed by LC-MS/MS with a Q-TOF high-resolution analyzer to characterize its phytochemical profile. An overview of the annotated compounds is shown in [Supplementary Fig. 3] (https://doi.org/10.38212/2224-6614.3591), and detailed LC-MS/MS parameters are listed in [Supplementary Fig. 1] (https://doi.org/10.38212/2224-6614.3591). In the positive ion mode [Supplementary Table 1] (https://doi.org/10.38212/2224-6614.3591), several isoflavones (biochanin A-D3, genistein, formononetin, 5,7-dihydroxy-4-hydroxyisoflavone, daidzein, dalspinin) and flavones (5,7-dihydroxy-3,6-dimethoxyflavone and 6,7-dihydroxy-3-(3,4-dimethoxyphenyl)-4H-1-benzopyran-4-one) were identified, along with putative compounds such as erucamide and phthalic acid derivatives. Peak area analysis indicated that genistein and biochanin A-D3 were among the most abundant constituents.

In the negative ion mode [Supplementary Table 1] (https://doi.org/10.38212/2224-6614.3591), several isoflavones (genistein, ermanin, daidzein, formononetin, pseudobaptigenin, cajanol), flavones (luteolin and 3,6,4′-trihydroxyflavone), and flavonoid glycosides (Kaempferol-3-sophoroside-7-glucoside and Pedunculosumoside G) were detected. These flavonoids are likely major active constituents of EECR95 and may underlie its therapeutic effects.

4. Discussion

This study evaluated the potential of ethanol extracts of CCR to improve atopic dermatitis (AD) through three different anti-inflammatory models: LPS-induced inflammation in macrophages (mTHP-1), MRSA-induced macrophage inflammation, and MRSA-induced keratinocyte (HaCaT) inflammation. The results demonstrated that EECR95 exhibits significant anti-inflammatory and antibacterial properties, supporting its potential use in AD treatment. The LC-MS/MS analysis revealed that EECR95 contains various isoflavones and flavones, known for their antibacterial and anti-inflammatory properties. Therefore, these compounds are considered the main active components in EECR95.

EECR95 extract demonstrated the highest potential for inhibiting SA among the CCR extracts, exhibiting the lowest MIC and MBC values (120, 225 μg/mL). Because stronger bactericidal agents may also damage skin cells, it is more appropriate for the development of commercial raw materials to select samples that inhibit bacterial growth while minimizing cytotoxicity to skin cells. Table 1 shows that ampicillin and genistein exhibit significantly greater antibacterial effects than EECR95. However, at concentrations below 100 μg/mL, EECR95 primarily inhibited cell proliferation without causing cytotoxicity in THP-1 cells, thereby offering greater safety for clinical applications.

The findings showed that EECR95 inhibited the proliferation of SA and MRSA in a dose-dependent manner. Notably, while Ampicillin was effective against SA, it showed no inhibitory effect on MRSA, highlighting the significance of EECR95 as an alternative treatment option. The IC_{50} values for EECR95 against SA and MRSA (93.25 μg/mL and 103.74 μg/mL, respectively) indicate that the extract has consistent antibacterial activity even against antibiotic-resistant strains. However, these data indicate that EECR95 exerts modest *in vitro* antibacterial activity against MRSA, which may not be sufficient on its own to achieve clinically meaningful effects *in vivo*.

In the anti-inflammatory experiments, we used non-cytotoxic concentrations of genistein and EECR95 in mTHP-1 cells ($\leq$10 and $\leq$ 40 μg/mL, respectively). These concentrations are closer to pharmacological than strictly physiological levels, as *in vitro* studies often require higher doses than those achievable through normal dietary intake or *in vivo* exposure to explore pharmacological potential and mechanisms. Thus, the concentrations used here are primarily of pharmacological relevance, serving to evaluate potential therapeutic effects and underlying molecular mechanisms rather than to directly mimic actual exposure levels in humans or animals.

The anti-inflammatory effects of EECR95 were evident in all three models. In the LPS-induced mTHP-1 model, EECR95 significantly reduced the production of pro-inflammatory cytokines, including IL-1β, IL-6, and TNF-α, in a dose-dependent manner. At a concentration of 40 μg/mL, EECR95 demonstrated superior inhibition of IL-1β and TNF-α compared to genistein, a known anti-inflammatory compound. This suggests that EECR95 may have a stronger and broader anti-inflammatory effect, potentially attributed to its bioactive compounds

月日知識庫

such as soy isoflavones (genistein, biochanin A, daidzein, and cajanol) [22].

The clinical physiological characteristics of AD are marked by significantly elevated levels of pro-inflammatory mediators, cytokines, histamine, tyrosine kinase, and oxidative stress. Flavonoids have also been proven as natural anti-inflammatory agents in the AD treatments [29]. Xu et al. [30] reported that genistein exhibits strong antipruritic and anti-inflammatory effects in ACD mice by inhibiting the production of pro-inflammatory cytokines and intracellular MAP2K2/ERK cell signaling, making genistein a potentially valuable candidate to improve skin conditions and systemic syndromes in the setting of contact dermatitis. LC-MS/MS analysis of EECR95 also revealed the presence of isoflavones (biochanin A, genistein, formononetin, 5,7-dihydroxy-4-hydroxyisoflavone, daidzein, dalspinin, ermanin, pseudobaptigenin, and cajanol), flavones (such as 5,7-dihydroxy-3,6-dimethoxyflavone, luteolin, and 3,6,4′-trihydroxyflavone), and flavonoid glycosides (such as kaempferol-3-sophoroside-7-glucoside and pedunculosumoside G). Thus, we speculated that the above compounds may contribute to the effects of EECR95.

In the MRSA-induced mTHP-1 inflammation model (direct stimulation), co-culturing mTHP-1 cells with MRSA for more than 1 h leads to a significant decrease in cell numbers. When the reaction time is limited to only 1 h, the induced inflammatory response is minimal and difficult to detect. In the direct stimulation model, EECR95 exhibited moderate inhibition of TNF-α production but did not significantly reduce IL-1β levels. However, if MRSA is first co-cultured with HaCaT cells for 12 h, and the cell-bacteria culture supernatant (which must be filtered to remove MRSA) is then used to react with THP-1 cells for 24 h, a greater amount of inflammatory factors can be induced. This model also more closely resembles the multi-stage inflammatory response in AD cellular models.

In the MRSA-induced HaCaT inflammation model, EECR95 effectively reduced the levels of IL-1β, IL-6, and TNF-α through indirect stimulation. At a concentration of 40 μg/mL, EECR95 achieved inhibition rates of 48.59%, 88.33%, and 86.97% for IL-1β, IL-6, and TNF-α, respectively. These results highlight the potential of EECR95 to mitigate keratinocyte-driven inflammation, which is a hallmark of AD pathophysiology [7,10].

SA, particularly MRSA, plays a critical role in the pathogenesis of AD by colonizing lesional and non-lesional skin, exacerbating skin inflammation, and being associated with increased disease severity [31]. MRSA attaches more efficiently to AD skin due to specific receptors and binding proteins (e.g., fibronectin and fibrinogen binding proteins) that increase the expression in the inflammatory environment of AD [32]. Once colonized, MRSA exacerbates AD by producing virulence factors (VFs) that act as superantigens, which trigger disproportionate immune responses and increased inflammation [32,33]. MRSA also secretes enzymes such as proteases and lipases, which degrade important skin barrier proteins, increase permeability, and facilitate the entry of other allergens and pathogens [34,35]. In addition, the ability of MRSA to form biofilms complicates eradication because biofilms resist antimicrobial agents and host immune responses, allowing colonization to persist [36]. These interactions highlight the importance of effectively inhibiting MRSA proliferation and colonization, as well as mitigating the associated immune dysregulation, to alleviate AD symptoms.

As found in much of the published literature, many evaluations of the ability of natural substances or their active ingredients to improve AD utilize the anti-proliferation of MRSA and reduce pro-inflammatory cytokines in keratinocytes, for example, Chamomile (*Matricaria chamomilla*) [37], Licorice (*Glycyrrhiza glabra*) [38], Turmeric (*Curcuma longa*) [39], Aloe Vera (*Aloe barbadensis*) [40] and Green Tea (*Camellia sinensis*) [41].

MRSA colonization on AD skin is particularly significant because it produces virulence factors, such as superantigens (e.g., staphylococcal enterotoxins), α-toxin, δ-toxin, and PSMs. These factors disrupt keratinocyte function, induce mast cell degranulation, and trigger the release of pro-inflammatory cytokines, including IL-1β, IL-6, and TNF-α [42].

The MRSA-induced HaCaT inflammation model used in this study closely mimics these processes, as keratinocytes exposed to MRSA exhibited elevated levels of these cytokines, which are central to AD pathogenesis. We simulated the colonization of MRSA on keratinocytes (HaCaT), which induced the production of pro-inflammatory factors (IL-1β, IL-8, IL-17, GM-CSF), toxins (PSMs, δ-toxins, TSLP), and ROS. Subsequently, macrophages (mTHP-1) were further induced to produce a more pronounced inflammatory response. This model is considered the most suitable for evaluating whether samples have the potential to improve AD. It also more closely recapitulates the situation in AD, in which keratinocytes exposed to external stimuli release a variety of alarmins and chemokines that subsequently activate dermal macrophages [43].

月日知識庫

The soy isoflavones in EECR95, such as genistein, may act as comparable active compounds. It has been reported that genistein significantly enhances the expression of key barrier proteins (FLG, Claudin-1, ZO-1), hydration factors (AQP3, HAS-1, HAS-2), and antimicrobial peptides (hBD3) in inflamed keratinocytes, and the effects of restoring filaggrin and hyaluronic acid synthase are better than dexamethasone [44]. Yuan et al. [45] reported that formononetin attenuated AD by upregulating tumor necrosis factor alpha-induced protein 3 (TNFAIP3) expression (which plays an important role in regulating immune and inflammatory responses as a negative regulator of NF-κB) *via* activation of protein-coupled estrogen receptor (GPER), thereby inhibiting the expression of pro-inflammatory factor TSLP. Thus, formononetin can also improve the airway allergic inflammatory response.

The therapeutic potential of EECR95 is further supported by its dual-action mechanism, which combines antibacterial, antioxidant (ROS scavenger) and anti-inflammatory effects. EECR95 offers a comprehensive approach to managing AD by addressing microbial dysbiosis and immune dysregulation.

The study further examined the mRNA expression levels of key pro-inflammatory mediators, including IL-1α, IL-17, and GM-CSF, in MRSA-stimulated HaCaT cells. EECR95 significantly suppressed the expression of these cytokines, with inhibition rates ranging from 52% to 67%. These findings suggest that EECR95 can modulate the inflammatory response at a transcriptional level, potentially by interfering with signaling pathways such as NF-κB and Nrf2, as previously reported [23]. This dual action—antibacterial and anti-inflammatory—positions EECR95 as a promising therapeutic candidate for AD.

EECR95 showed no detectable cytotoxicity to THP-1–derived macrophages and MRSA-stimulated THP-1 cells at concentrations up to 100 μg/mL, indicating a favorable safety profile within this concentration range. However, the MIC and MBC values against SA (120 and 225 μg/mL, respectively) are higher than the concentrations tested for cytotoxicity. Therefore, further studies are required to evaluate the safety of EECR95 at bacteriologically effective doses, particularly in skin-relevant cell types.

One limitation of this study is that only EECR95 was investigated in depth. Although EECR95 showed the strongest bioactivity in our previous work, this focus may have caused us to overlook hydrophilic compounds (e.g., polysaccharides) that are more abundant in higher-polarity extracts (EECR50 or EECR75). Future studies will therefore systematically evaluate these more hydrophilic extracts and their fractions in AD models to better define the therapeutic potential of this botanical extract.

In summary, we believe that the decrease in AMP and FDP in AD leads to increased trans-epidermal water loss (TEWL) and elevated pH in the epidermis compared to normal skin. This condition easily results in epidermal barrier dysfunction, making AD patients more prone to itching and skin barrier damage, which subsequently triggers MRSA colonization and proliferation. Subsequently, the secretion of PSMs, δ-toxins, and TSLP, along with the production of ROS, stimulated keratinocytes to release pro-inflammatory factors, which in turn activated macrophages to amplify the inflammatory response. We found that EECR95 possesses antibacterial, anti-inflammatory, and antioxidant properties, which can inhibit keratinocytes from producing pro-inflammatory factors that would otherwise induce macrophages to produce excessive inflammatory cytokines, thereby alleviating severe inflammatory symptoms in AD patients. We speculate that this ability is related to the presence of flavonoids, isoflavones, and flavonoid glycosides in EECR95. Additionally, EECR95 showed no detectable cytotoxicity at concentrations up to 100 and 40 μg/mL in THP-1 and mTHP-1 cells, respectively, as assessed by MTT and Trypan blue assays. These findings suggest a favorable preliminary safety profile for EECR95. However, MTT and Trypan blue mainly reflect metabolic activity and membrane integrity and may not detect subtle cytotoxic effects. Further analyses (e.g., apoptosis markers, cell-cycle profiling, and functional assays) will therefore be needed to more fully characterize the impact of EECR95 on cytotoxicity and cellular function.

Funding

This research was funded by the Council of Agriculture, Executive Yuan of the Republic of China (ROC), Taiwan, grant number 114AS-1.7.1-FD-03, and partly funded by the Taichung Veterans General Hospital Project, Da-Yeh University, Taiwan, R.O.C., under grant number TCVGH-DYU1128302, 1138302 and 1148301 and Ministry of Education awards and subsidies to Chienkuo Technology University (CTU-110-RP-002-B-02).

Conflicts of interest

The authors declare no conflict of interest.

月旦知識庫

References

[1] Kim J, Kim BE, Ahn K, Leung DYM. Interactions between atopic dermatitis and *Staphylococcus aureus* infection: clinical implications. Allergy Asthma Immunol Res 2019;11(5):593–603.

[2] Kim BE, Leung DY. Significance of skin barrier dysfunction in atopic dermatitis. Allergy Asthma Immunol Res 2018;10:207–15.

[3] Breuer K, Häussler S, Kapp A, Werfel T. Staphylococcus aureus: colonizing features and influence of antibacterial treatment in adults with atopic dermatitis. Br J Dermatol 2002;147:55–61.

[4] Kim BS, Kim JY, Lim HJ, Lee WJ, Lee SJ, Kim JM, et al. Colonizing features of *Staphylococcus aureus* in early childhood atopic dermatitis and in mothers: a cross-sectional comparative study done at four kindergartens in Daegu, South Korea. Ann Allergy Asthma Immunol 2011;106:323–9.

[5] Jagadeesan S, Kurien G, Divakaran MV, Sadanandan SM, Sobhanakumari K, Sarin A. Methicillin-resistant Staphylococcus aureus colonization and disease severity in atopic dermatitis: a cross-sectional study from South India. Indian J Dermatol Venereol Leprol 2014;80:229–34.

[6] Petry V, Lipnharski C, Bessa GR, Silveira VB, Weber MB, Bonamigo RR, et al. Prevalence of community-acquired methicillin-resistant *Staphylococcus aureus* and antibiotic resistance in patients with atopic dermatitis in Porto Alegre, Brazil. Int J Dermatol 2014;53:731–5.

[7] Kim J, Kim BE, Leung DY. Pathophysiology of atopic dermatitis: clinical implications. Allergy Asthma Proc 2019;40:84–92.

[8] Ong PY, Leung DY. Bacterial and viral infections in atopic dermatitis: a comprehensive review. Clin Rev Allergy Immunol 2016;51:329–37.

[9] Clausen ML, Edslev SM, Andersen PS, Clemmensen K, Krogfelt KA, Agner T. *Staphylococcus aureus* colonization in atopic eczema and its association with filaggrin gene mutations. Br J Dermatol 2017;177:1394–400.

[10] Geoghegan JA, Irvine AD, Foster TJ. *Staphylococcus aureus* and atopic dermatitis: a complex and evolving relationship. Trends Microbiol 2018;26:484–97.

[11] Howell MD, Gallo RL, Boguniewicz M, Jones JF, Wong C, Streib JE, et al. Cytokine milieu of atopic dermatitis skin subverts the innate immune response to vaccinia virus. Immunity 2006;24:341–6.

[12] Jungersted JM, Hellgren LI, Jemec GB, Agner T. Lipids and skin barrier function—a clinical perspective. Contact Dermat 2008;58:255–62.

[13] Berdyshev E, Goleva E, Bronova I, Dyjack N, Rios C, Jung J, et al. Lipid abnormalities in atopic skin are driven by type 2 cytokines. JCI Insight 2018;3:98006.

[14] Mayo B, Rachid CT, Alegría A, Leite AM, Peixoto RS, Delgado S. Impact of next generation sequencing techniques in food microbiology. Curr Genom 2014;15:293–309.

[15] Peschel A, Otto M. Phenol-soluble modulins and staphylococcal infection. Nat Rev Microbiol 2013;11:667–73.

[16] Akande K, Abubakar M, Adegbola T, Bogoro S, Doma U. Chemical evaluation of the nutritive quality of pigeon pea [*Cajanus cajan* (L.) Millsp.]. Int J Poult Sci 2010;9:63–5.

[17] Ganapathy K, Gnanesh B, Byre Gowda M, Venkatesha S, Gomashe SS, Channamallikarjuna V. AFLP analysis in pigeonpea (*Cajanus cajan* (L.) Millsp.) revealed close relationship of cultivated genotypes with some of its wild relatives. Genet Resour Crop Evol 2011;58:837–47.

[18] Orni PR, Ahmed SZ, Monefa M, Khan T, Dash PR. Pharmacological and phytochemical properties of *Cajanus cajan* (L.) Huth. (Fabaceae): a review. Int J Pharm Sci Res 2018;3:27–37.

[19] Pal D, Mishra P, Sachan N, Ghosh AK. Biological activities and medicinal properties of *Cajanus cajan* (L.) Millsp. J Adv Pharm Technol Res 2011;2(4):207–14.

[20] Yang SE, Vo TLT, Chen CL, Yang NC, Chen CI, Song TY. Nutritional composition, bioactive compounds and functional evaluation of various parts of *Cajanus cajan* (L.) Millsp. Agriculture 2020;10(11):558.

[21] Yang SE, Lin YF, Liao JW, Chen JT, Chen CL, Chen CI, et al. Insulin sensitizer and antihyperlipidemic effects of *Cajanus cajan* (L.) Millsp. root in methylglyoxal-induced diabetic rats. Chin J Physiol 2022;65:125–35.

[22] Vo TLT, Cai XM, Liao JW, Huang LG, Chen CL, Wu CH, et al. Safety assessment and hepatic-renal protection of *Cajanus cajan* (L.) Millsp. roots and its soy isoflavone contents analysis. Nutrients 2023;15(18):3963.

[23] Vo TLT, Yang NC, Yang SE, Chen CL, Wu CH, Song TY. Antioxidant and anti-inflammatory effects of extracts from *Cajanus cajan* (L.) Millsp. roots. Chin J Physiol 2020;63(3):137–48.

[24] Makade CS, Shenoi PR, Bhongade BA, Shingane SA, Ambulkar PC, Shewale AM. Estimation of MBC: MIC ratio of herbal extracts against common endodontic pathogens. J Pharm BioAllied Sci 2024;16(Suppl 2):S1414–6.

[25] Arullappan S, Zakaria Z, Basri DF. Preliminary screening of antibacterial activity using crude extracts of Hibiscus rosa sinensis. Trop Life Sci Res 2009;20(2):109–18.

[26] Koganti R, Yadavalli T, Shukla D. *In vitro* protocol for the optimal induction of inflammation in human monocyte cell lines. STAR Protoc 2023;4(2):102342.

[27] Lee MF, Wang NM, Chen YH, Wu CS, Lee MH, Chu YW. An atopic dermatitis-like murine model by skin-brushed cockroach per a 2 and oral tolerance induction by *Lactococcus lactis*-derived per a 2. PLoS One 2023;18(9):e0291162.

[28] López-Fernández O, Domínguez R, Pateiro M, Munekata PES, Rocchetti G, Lorenzo JM. Determination of polyphenols using liquid chromatography-tandem mass spectrometry technique (LC-MS/MS): a review. Antioxidants (Basel) 2020;9(6):479.

[29] Zawawi NA, Ahmad H, Madatheri R, Fadilah NIM, Maarof M, Fauzi MB. Flavonoids as natural anti-inflammatory agents in the atopic dermatitis treatment. Pharmaceutics 2025;17(2):261.

[30] Xu J, Xiong H, Zhao Z, Luo M, Ju Y, Yang G, et al. Genistein suppresses allergic contact dermatitis through regulating the MAP2K2/ERK pathway. Food Funct 2021;12(10):4556–69.

[31] Shi B, Leung DYM, Taylor PA, Li H. Methicillin-Resistant Staphylococcus aureus colonization is associated with decreased skin commensal bacteria in atopic dermatitis. J Invest Dermatol 2018;138(7):1668–71.

[32] Foster TJ, Geoghegan JA, Ganesh VK, Höök M. Adhesion, invasion and evasion: the many functions of the surface proteins of *Staphylococcus aureus*. Nat Rev Microbiol 2014;12:49–62.

[33] Berube BJ, Wardenburg JB. *Staphylococcus aureus* α-toxin: nearly a century of intrigue. Toxins 2013;5:1140–66.

[34] Nakatsuji T, Chen TH, Two AM, Chun KA, Narala S, Geha RS, et al. *Staphylococcus aureus* exploits epidermal barrier defects in atopic dermatitis to trigger cytokine expression. J Invest Dermatol 2016;136:2192–200.

[35] Sonesson A, Przybyszewska K, Eriksson S, Mörgelin M, Kjellström S, Davies J, et al. Identification of bacterial biofilm and the *Staphylococcus aureus* derived protease, staphopain, on the skin surface of patients with atopic dermatitis. Sci Rep 2017;7:8689.

[36] Di DEG, Cavallo I, Capitanio B, Ascenzioni F, Pimpinelli F, Morrone A, et al. *Staphylococcus aureus* and the cutaneous microbiota biofilms in the pathogenesis of atopic dermatitis. Microorganisms 2019;7:301.

[37] El Mihyaoui A, Esteves da Silva JCG, Charfi S, Candela Castillo ME, Lamarti A, Arnao MB. Chamomile (*Matricaria chamomilla* L.): a review of ethnomedicinal use, phytochemistry and pharmacological uses. Life 2022;12(4):479.

[38] Lee SH, Bae IH, Choi H, Choi HW, Oh S, Marinho PA, et al. Ameliorating effect of dipotassium glycyrrhizinate on an IL-4- and IL-13-induced atopic dermatitis-like skin-equivalent model. Arch Dermatol Res 2019;311:131–40.

[39] So-In C, Sunthamala N. Treatment efficacy of Thunbergia laurifolia, Curcuma longa, Garcinia mangostana, and

月日知識庫

Andrographis paniculata extracts in *Staphylococcus aureus*-induced rabbit dermatitis model. Vet World 2022;15(1): 188–97.

[40] Maan SA, Faiesal AA, Gamar GM, Dougdoug NKE. Efficacy of bacteriophages with Aloe vera extract in formulated cosmetics to combat multidrug-resistant bacteria in skin diseases. Sci Rep 2025;15:4335.

[41] Huang Z, Zhang L, Xuan J, Zhao T, Peng W. Antibacterial and antiallergic effects of three tea extracts on histamine-induced dermatitis. Pharmaceuticals 2024;17(9):1181.

[42] Nakatsuji T, Chen TH, Narala S, Chun KA, Two AM, Yun T, et al. Antimicrobials from human skin commensal bacteria protect against *Staphylococcus aureus* and are deficient in atopic dermatitis. Sci Transl Med 2017;9: eaah4680.

[43] Humeau M, Boniface K, Bodet C. Cytokine-mediated crosstalk between keratinocytes and T cells in atopic dermatitis. Front Immunol 2022;13:801579.

[44] Mohammad S, Valappil AK, Karim MR, Iqbal S, Yang DC, Chen C, et al. Protective roles of genistein and icaritin in skin barrier integrity and hydration in an atopic dermatitis model. Eur J Integr Med 2025;76:102483.

[45] Yuan W, Chen Y, Zhou Y, Bao K, Yu X, Xu Y, et al. Formononetin attenuates atopic dermatitis by upregulating A20 expression via activation of G protein-coupled estrogen receptor. J Ethnopharmacol 2021;266:113397.